

Equation of state for pure SU(3) gauge theory with renormalization group improved action

CP-PACS Collaboration

¹M. Okamoto, ²A. Ali Khan, ¹S. Aoki, ^{1,2}R. Burkhalter, ²S. Ejiri, ³M. Fukugita, ⁴S. Hashimoto, ^{1,2}N. Ishizuka,
^{1,2}Y. Iwasaki, ^{1,2}K. Kanaya, ²T. Kaneko, ⁵Y. Kuramashi*, ²T. Manke, ²K. Nagai, ⁴M. Okawa, ^{1,2}A. Ukawa,
^{1,2}T. Yoshié

¹*Institute of Physics, University of Tsukuba,
Tsukuba, Ibaraki 305-8571, Japan*

²*Center for Computational Physics, University of Tsukuba,
Tsukuba, Ibaraki 305-8577, Japan*

³*Institute for Cosmic Ray Research, University of Tokyo,
Tanashi, Tokyo 188-8502, Japan*

⁴*High Energy Accelerator Research Organization (KEK),
Tsukuba, Ibaraki 305-0801, Japan*

⁵*Department of Physics, Washington University,
St. Louis, Missouri 63130, USA
(September 19, 2018)*

A lattice study of the equation of state for pure SU(3) gauge theory using a renormalization-group (RG) improved action is presented. The energy density and pressure are calculated on a $16^3 \times 4$ and a $32^3 \times 8$ lattice employing the integral method. Extrapolating the results to the continuum limit, we find the energy density and pressure to be in good agreement with those obtained with the standard plaquette action within the error of 3–4%.

arXiv:hep-lat/9905005v2 14 Sep 1999

*On leave from Institute of Particle and Nuclear Studies, High Energy Accelerator Research Organization(KEK), Tsukuba, Ibaraki 305-0801, Japan

I. INTRODUCTION

At sufficiently high temperatures, the quark-confinement property of QCD is expected to be lost so that hadrons dissolve into a plasma of quarks and gluons. This quark-gluon plasma state must have existed in the early Universe, and its experimental detection is being actively pursued through relativistic heavy-ion collisions. Basic information that is required to explore physical phenomena in the quark-gluon plasma is its equation of state, namely the energy density and pressure as a function of temperature. For this reason a number of lattice QCD studies of equation of state have been made [1]. An important progress in this effort is the recent work of the Bielefeld group [2] in which a systematic continuum extrapolation was carried out for the equation of state for pure SU(3) gauge theory. Using the standard plaquette action, they calculated bulk thermodynamic quantities on lattices with the temporal extent $N_t = 4, 6$ and 8 , and extrapolated the results to the continuum limit $N_t \rightarrow \infty$, assuming that the data at $N_t = 6$ and 8 follow the leading extrapolation formula.

To understand the quark gluon plasma in the real world, this work has to be extended to full QCD with dynamical quarks. This is a difficult task due to significant increase of the amount of computations needed for full QCD simulations. One approach to lessen the computational cost is to employ improved actions designed to have reduced lattice cut-off effects, and hence should allow reliable continuum extrapolation from coarser lattice spacings compared to the case for the standard unimproved actions. Thermal properties of several improved pure gauge actions have already been studied [3–6]. At present, however, no extrapolation of thermodynamic quantities to the continuum limit has been made with improved actions.

In this article we report on our study of the continuum limit of equation of state for pure SU(3) gauge theory with an improved action determined from an approximate renormalization-group argument [7]. Simulations are carried out on $16^3 \times 4$ and $32^3 \times 8$ lattices, and the energy density and pressure are calculated by the integral method [8]. We find that the results extrapolated to the continuum limit agree well with those obtained from the standard action in Ref. [2]. This provides us with a cross-check of the final results in the continuum limit, and also provide support for the validity of assumptions behind the extrapolation procedures.

This paper is organized as follows. In Section II, we summarize the basic formulation and our notations. Some details of our simulations are given in Section III. We define our choice of the temperature scale in terms of the string tension in Section IV, and examine scaling of the critical temperature in Section V. In Section VI we present our results for equation of state obtained at $N_t = 4$ and 8 , and their continuum extrapolation. A comparison of our results with those obtained from the standard action is also made. In Section VII we briefly discuss results obtained with the operator method [9]. We end with a brief conclusion in Section VIII.

II. METHOD

The partition function of a finite temperature SU(3) lattice gauge theory is defined by

$$Z = \int [dU] e^{\beta S_g}, \quad (1)$$

where $\beta = 6/g^2$ is the bare gauge coupling, and S_g the lattice gauge action. Denoting the $k \times l$ Wilson loop in the (μ, ν) -plane at a site x as $W_{\mu\nu}^{k \times l}(x) = \frac{1}{3} \text{ReTr} \left[\prod_{k \times l \text{ loop}} U \right]$, the renormalization group (RG) improved gauge action we use is given by [7]

$$S_g = c_0 \sum_{x, \mu < \nu} W_{\mu\nu}^{1 \times 1}(x) + c_1 \sum_{x, \mu, \nu} W_{\mu\nu}^{1 \times 2}(x) \quad (2)$$

with $c_0 = 1 - 8c_1$ and $c_1 = -0.331$. On a lattice with a size $N_s^3 \times N_t$ and the lattice spacing a , the temperature T and physical volume V of the system are given respectively by

$$T = 1/(N_t a), \quad V = (N_s a)^3. \quad (3)$$

We calculate the energy density ϵ and pressure p using the integral method [8]. For a large homogeneous system, the pressure is related to the free energy density f through

$$p = -f = \frac{T}{V} \ln Z. \quad (4)$$

Using an identity $\frac{\partial}{\partial\beta} \ln Z = \langle S_g \rangle$, we then have

$$\frac{p}{T^4} \Big|_{\beta_0}^{\beta} = \int_{\beta_0}^{\beta} d\beta' \Delta S, \quad (5)$$

where

$$\Delta S \equiv N_t^4 (\langle S \rangle_T - \langle S \rangle_0), \quad (6)$$

with $\langle S \rangle_T$ the expectation value of the action density $S = S_g/N_s^3 N_t$ at temperature T . The zero-temperature expectation value $\langle S \rangle_0$ is introduced to subtract the vacuum contribution, which is conventionally computed on a symmetric lattice with the same spatial volume $N_s^3 \times N_s$. Once the pressure is known, the energy density can be computed using

$$\frac{\epsilon - 3p}{T^4} = T \frac{d\beta}{dT} \Delta S, \quad (7)$$

where

$$T \frac{d\beta}{dT} = -a \frac{d\beta}{da} \equiv \beta(g) \quad (8)$$

is the QCD beta-function.

III. SIMULATIONS

The fundamental quantity used in the integral method is the action difference ΔS defined by (6). In order to calculate $\langle S \rangle_T$ and $\langle S \rangle_0$, we need to simulate both asymmetric ($N_s^3 \times N_t$) and symmetric ($N_s^3 \times N_s$) lattices. The spatial lattice size N_s should be sufficiently large to suppress finite size effects. Past finite-size studies [10,11,3] suggest that the condition $N_s/N_t \gtrsim 3$ is the minimum requirement. As with the work of the Bielefeld group for the plaquette action [2], we choose $N_s/N_t = 4$ and perform simulations on $16^3 \times 4$ and $32^3 \times 8$ lattices as well as on 16^4 and 32^4 lattices for a set of values of β around and above the critical point.

Gauge fields are updated by the pseudo-heat-bath algorithm with five hits, followed by four over-relaxation sweeps; the combination of these updates is called an iteration. We always start from the completely ordered configuration, and perform 20 000 to 36 000 iterations after thermalization on asymmetric lattices, and about 10 000 iterations on symmetric lattices. We find these number of iterations to be sufficient for a statistical accuracy of 2–3% or better for the value of ΔS . The statistics of our runs are compiled in Table I.

We measure Wilson loops and Polyakov loop at every iteration. Errors are determined by the jack-knife method. The typical bin size dependence of the jack-knife error for the action density is shown in Fig. 1. The errors are almost constant over a wide range of bin sizes, and we adopt the bin size of 1000 iterations for asymmetric lattices and 500 on symmetric lattices.

In Table II we list the expectation value of the action density $\langle S \rangle_T$ calculated on asymmetric lattices of size $16^3 \times 4$ and $32^3 \times 8$ and that for $\langle S \rangle_0$ on symmetric lattices of size 16^4 and 32^4 .

IV. TEMPERATURE SCALE

In order to determine the temperature $T = 1/(N_t a(\beta))$, we need to compute the lattice spacing a as a function of the gauge coupling β . We use the string tension of static quark potential to fix the scale of this relation. In Table III we compile results for the dimensionless string tension $a\sqrt{\sigma}$ obtained with the RG-improved action [3,12]. We fit these results by an ansatz proposed by Allton [13],

$$(a\sqrt{\sigma})(\beta) = f(\beta) (1 + c_2 \hat{a}(\beta)^2 + c_4 \hat{a}(\beta)^4 + \dots)/c_0, \quad \hat{a}(\beta) \equiv \frac{f(\beta)}{f(\beta_1)}, \quad (9)$$

where $f(\beta)$ is the two-loop scaling function of SU(3) gauge theory,

$$f(\beta = 6/g^2) \equiv (b_0 g^2)^{-\frac{b_1}{2b_0^2}} \exp\left(-\frac{1}{2b_0 g^2}\right), \quad b_0 = \frac{11}{(4\pi)^2}, \quad b_1 = \frac{102}{(4\pi)^4}, \quad (10)$$

and $c_n (n = 2, 4, \dots)$ parameterize deviations from the two-loop scaling. Truncating the power corrections at $n = 4$ and choosing $\beta_1 = 2.40$, we obtain from this fit,

$$c_0 = 0.524(15), c_2 = 0.274(76), c_4 = 0.105(36) \quad (11)$$

with $\chi^2/dof = 0.356$ for 4 degrees of freedom. As shown in Fig.2 the fit curve reproduces the data very well.

With this parametrization, the temperature in units of the critical temperature T_c is given by

$$\frac{T}{T_c} = \frac{(a\sqrt{\sigma})(\beta_c)}{(a\sqrt{\sigma})(\beta)}. \quad (12)$$

with β_c the critical coupling. The beta-function is obtained by differentiating the left hand side of (9) with respect to the lattice spacing a , keeping σ constant.

V. CRITICAL TEMPERATURE

We determine the critical coupling $\beta_c(N_t, N_s)$ for the deconfinement transition on an $N_s^3 \times N_t$ lattice by the peak location of the susceptibility χ of the Z(3)-rotated Polyakov line. The values of β_c for $N_t = 3, 4, 6$ have been reported in Ref. [3]. In order to compute β_c for $N_t = 8$, we perform an additional simulation of 24 000 iterations at $\beta = 2.710$ on a $32^3 \times 8$ lattice. The β dependence of χ is calculated by the spectral density method [14]. We estimate the error by the jack-knife method with the bin-size of 2000 iterations. The values of $\beta_c(N_t, N_s)$ for finite N_s are summarized in the second column of Table IV.

Calculating the critical temperature requires an extrapolation of $\beta_c(N_t, N_s)$ toward infinite spatial size $N_s \rightarrow \infty$ for each N_t . For the first-order transition of the pure gauge system, the spatial volume dependence of $\beta_c(N_t, N_s)$ is expected to follow [2]

$$\beta_c(N_t, N_s) = \beta_c(N_t, \infty) - c(N_t) \frac{N_t^3}{N_s^3}. \quad (13)$$

It has been reported in Ref. [3] that results for $N_t = 3$ and 4 reasonably satisfy (13) with $c(N_t) = 0.122(54)$ for $N_t = 3$ and 0.133(63) for $N_t = 4$. An approximate scaling of the coefficient $c(N_t)$ motivates us to apply (13) for $N_t = 6$ (as was made in Ref. [3]) and also for $N_t = 8$, adopting the value 0.133(63) for the coefficient. Substituting values of $\beta_c(N_t, \infty)$ in the parametrization of the string tension (9), we calculate $T_c/\sqrt{\sigma} = 1/(N_t a \sqrt{\sigma})$. We tabulate results of this analysis in the third and fourth column of Table IV.

In Fig. 3 we plot the results for $T_c/\sqrt{\sigma}$ as a function of $1/N_t^2$ (filled circles). Also shown are the values previously reported in Ref. [3] (open circles) and those for the plaquette action from Ref. [16] (open squares). A slight difference between the present results and those from Ref. [3] for the same action stems from the fact that an exponential ansatz $\sqrt{\sigma}a = A \exp(-B\beta)$ with fit parameters A and B was adopted in the previous work, which deviates from the parametrization (9). We think that the present parametrization gives a better estimate of σ , being theoretically consistent with the asymptotic scaling behavior for large β . The results for the plaquette action is obtained with a parametrization [15]

$$(a\sqrt{\sigma})(\beta) = f(\beta) (1 + 0.2731 \hat{a}(\beta)^2 - 0.01545 \hat{a}(\beta)^4 + 0.01975 \hat{a}(\beta)^6) / 0.01364 \quad (14)$$

with $\beta_1 = 6.0$.

We observe that the new value of $T_c/\sqrt{\sigma}$ for the RG-improved action for $N_t = 8$ is consistent with the previous results for $N_t = 3, 4, 6$ [3]. The difference in this ratio obtained for the two actions, however, still remains. Making a quadratic extrapolation in $1/N_t$, we find $T_c/\sqrt{\sigma} = 0.650(5)$ for the RG action, which is 3% higher than the value 0.630(5) for the plaquette action [16]. A possible origin of the discrepancy is systematic uncertainties in the determination of the string tension for the two actions, which differ in details. We consider that checking an agreement beyond a few percent accuracy, as is needed here, would require the generation and analyses of potential data over the relevant range of lattice spacings in a completely parallel manner for the two actions, which is beyond the scope of the present work.

VI. EQUATION OF STATE

A. Results for RG-improved action

Our results for ΔS at $N_t = 4$ and 8 are shown in Fig. 4. In order to integrate ΔS in terms of β to obtain the pressure, we have to make an interpolation of the data points. At large β where $T \geq 2T_c$ is satisfied, we fit the points by a perturbative ansatz,

$$\Delta S = \frac{a_2}{\beta^2} + \frac{a_3}{\beta^3} + \frac{a_4}{\beta^4} + \dots, \quad (15)$$

truncating the series at the order β^{-4} . The absence of the linear term in perturbation theory can be checked easily. For ΔS at lower β -values corresponding to $T \leq 2T_c$, we perform a cubic spline fit with the requirement that the curve smoothly joins to the large- β fit curve at $T = 2T_c$. The interpolation curves are shown in Fig. 4.

We use these curves to evaluate the integral for pressure in (5). The lower limit of integration is chosen to be $\beta_0 = 2.20$ ($N_t = 4$) and 2.63 ($N_t = 8$). The results are shown by solid lines in Fig. 5. Combining these results for p with those for $\epsilon - 3p$ computed using (7), we also obtain the energy density ϵ , which we show in Fig. 6.

The statistical error $\delta p(T)$ for the pressure, plotted at representative points in Fig. 5, is evaluated from the contributions $\delta_i p(T)$ at each simulation point β_i which is estimated by the jack-knife method. Since simulations at different β_i are statistically independent, we compute the final error by the naive error-propagation rule, $\delta p(T) = \sqrt{\sum_i \delta p_i(T)^2}$, summing up all the contributions from β_i smaller than β corresponding to the temperature T . The error $\delta \epsilon(T)$ of the energy density is calculated by quadrature from the error of $3\delta p(T)$ and that for $\epsilon(T) - 3p(T)$, the latter being proportional to the error of ΔS .

We observe in Figs. 5 and 6 that the energy density and pressure exhibit a sizable increase between $N_t = 4$ and 8. This increase is opposite to the trend for the plaquette action, but it is consistent with the prediction of the leading order perturbative result shown by horizontal lines at the right of the figure. The values from the integral method, however, overshoot those from perturbation theory toward high temperatures, particularly for $N_t = 4$ for which the perturbative value is quite small. We discuss this point further in Sec. VII.

We now extrapolate the results for energy density and pressure to the continuum limit $N_t \rightarrow \infty$. The RG-improved gauge action has lattice discretization errors of $O(a^2)$. Therefore, at a fixed temperature in physical units, we expect deviations of thermodynamic quantities from the continuum limit to be $O(1/N_t^2)$:

$$\left(\frac{\mathcal{F}}{T^4}\right)_{N_t} = \left(\frac{\mathcal{F}}{T^4}\right)_{\text{cont}} + \frac{c_{\mathcal{F}}(T)}{N_t^2}, \quad \mathcal{F} = p, \epsilon. \quad (16)$$

Extrapolating the results for ϵ and $3p$ at $N_t = 4$ and 8 with this form, we obtain the continuum predictions drawn by solid lines in Fig. 7.

B. Comparison with results for the plaquette action

We compare our results with those of the Bielefeld group obtained with the plaquette action [2]. Care is needed in this comparison since they used a scheme different from ours to fix the temperature scale: their scheme is based on the requirement that the critical temperature T_c is independent of the temporal size N_t .

Since a difference in the scale can sizably affect results for thermodynamic quantities [17], we first examine the possible influence of this difference. For this purpose we reanalyze the raw data of Ref. [2] for the action density employing the scale parametrization (14). The results for p and ϵ are shown by solid lines in Fig. 8 for the temporal sizes $N_t = 6$ and 8 used by the Bielefeld group for the continuum extrapolation. Compared with their original results, drawn by dashed lines, the influence of the scale determination is well within the statistical error of 1-3%.

We extrapolate the pressure and energy density obtained with the scale (14) to the continuum limit according to (16). This leads to the dash-dotted curves shown in Fig. 7. Errors are evaluated in the same way as for the case of the RG-improved action. We observe that the curves for the RG-improved action (solid lines) and those for the plaquette action (dash-dotted lines) are in good agreement, within the error of 3-4%, over the entire temperature interval shown. This is highly non-trivial since results for the two actions differ significantly at finite lattice spacings.

In Fig. 9 we compare the pressure at $N_t = 4$ from the two actions to the result in the continuum limit. We note that the continuum results for the RG-improved action are approached from below, while those for the plaquette action from above. We also find that the magnitude of deviation from the continuum limit is comparable for both

actions. The form of the RG-improved action we employed is determined so as to best approximate the renormalized trajectory after a few RG transformations, within those limited actions with a maximum of 6-link loops. Therefore, low-momentum modes, with a momenta smaller than the inverse of several lattice spacings, are improved. On the other hand, a momentum scale which is significant at high temperatures is $T = 1/N_t a$ on finite- N_t lattices. From Fig. 9, it appears to be required to add further terms in the action in order to reduce the cut-off effects for high-momentum modes with momentum $\gtrsim 1/4a$, thereby improving the behavior of the pressure at high temperatures on $N_t = 4$ lattices.

VII. COMPARISON WITH RESULTS WITH OPERATOR METHOD

In Sec. VIA we noted that the pressure and energy density calculated by the integral method exceed the values corresponding to the perturbative high temperature limit. This is a puzzling result, especially for pressure; while p/T^4 has to decrease at high temperatures to agree with the perturbative result, we expect it to be an increasing function of temperature since it is given by an integral of ΔS which is generally positive. The discrepancy is particularly large for $N_t = 4$ for which the leading order perturbative results on the lattice are quite small compared to those in the continuum as first noted in Ref. [18]. In Table V we list the perturbative value of pressure on a $N_s^3 \times N_t$ lattice in units of the free gluon gas value in the continuum for $N_t = 4-12$ for the RG-improved and plaquette actions.

In order to further examine this problem, we calculate thermodynamic quantities in an alternative way using the formulae of the operator method [9] given by

$$\frac{\epsilon}{T^4} = \frac{18}{g^2} N_t^4 [c_s(g)(\langle S_s \rangle - \langle S \rangle_0) - c_t(g)(\langle S_t \rangle - \langle S \rangle_0)], \quad (17)$$

$$\frac{p}{T^4} = \frac{1}{3} \frac{\epsilon}{T^4} - N_t^4 \beta(g) [\langle S_s + S_t \rangle - 2\langle S \rangle_0], \quad (18)$$

where S_s and S_t are the spatial and temporal part of the action density, and the asymmetry coefficients are defined by

$$c_s(g) = 1 - g^2 \left. \frac{dg_s^{-2}}{d\xi} \right|_{\xi=1}, \quad c_t(g) = 1 + g^2 \left. \frac{dg_t^{-2}}{d\xi} \right|_{\xi=1}. \quad (19)$$

The one-loop values of the asymmetry coefficients for the plaquette action have been long known [19], and preliminary values for the RG-improved action have recently been reported [20].

We compare results for the energy density and pressure from the integral method and the operator method with one-loop asymmetry coefficients in Fig. 10 for $N_t = 4$ and 8. For both types of actions, the values for the operator method lie above those for the integral method, and the difference diminishes with increasing N_t . For $N_t = 4$ for the RG-improved action, in particular, we do not observe any indication of decrease toward the perturbative high temperature limit, both with the integral and operator methods, at least within the temperature range where we have results.

A possible source of the discrepancy is breakdown of perturbation theory due to the infrared divergence [21] of the theory. In the continuum there are non-perturbative contributions to free energy beyond 3-loop level. This problem should also exist on the lattice, and the magnitude of non-perturbative contributions may vary depending on the choice of lattice actions.

VIII. CONCLUSIONS

In this article we have presented results on the equation of state for a pure SU(3) gauge theory obtained with an RG-improved gauge action. The continuum result for the energy density and pressure show an agreement with the results of the Bielefeld group for the plaquette action within the error of 3–4%. This provides a concrete support for the expectation that continuum results are insensitive to the choice of lattice actions.

We also found that the energy density and pressure for finite N_t overshoot the perturbative high temperature limit. Understanding the origin of this behavior shall be explored in the future.

ACKNOWLEDGEMENTS

We thank S. Sakai for communications on the asymmetry coefficients for the RG-improved action, F. Karsch for allowing us to reproduce their results in Fig. 8, and H.P. Shanahan for useful comments. Valuable discussions with B. Petersson and F. Karsch are gratefully acknowledged. Numerical simulations for the present work have been carried out with the CP-PACS facility at the Center for Computational Physics of the University of Tsukuba. This work is supported in part by Grants-in-Aid of the Ministry of Education (Nos. 6768, 6769, 7034, 09304029, 10640246, 10640248). AAK and TM are supported by the JSPS Research for Future Program. MO, SE and KN are JSPS Research Fellows.

- [1] For reviews, see, E. Laermann, Nucl. Phys. B (Proc. Suppl.) 63 (1998) 114; A. Ukawa, Nucl. Phys. B (Proc. Suppl.) 53 (1997) 106.
- [2] G. Boyd, J. Engels, F. Karsch, E. Laermann, C. Legeland, M. Lütgemeier and B. Petersson, Nucl. Phys. B469 (1996) 419.
- [3] Y. Iwasaki, K. Kanaya, T. Kaneko, and T. Yoshié, Phys. Rev. D56 (1997) 151.
- [4] F. Beinlich, F. Karsch and E. Laermann, Nucl. Phys. B462 (1996) 415.
- [5] F. Beinlich, F. Karsch and A. Peikert, Phys. Lett. B390 (1997) 268.
- [6] A. Papa, Nucl. Phys. B478 (1996) 335.
- [7] Y. Iwasaki, Nucl. Phys. B258 (1985) 141; Univ. of Tsukuba report UTHEP-118 (1983), unpublished.
- [8] J. Engels, J. Fingberg, F. Karsch, D. Miller and M. Weber, Phys. Lett. B 252 (1990) 625.
- [9] J. Engels, F. Karsch, I. Montvay and H. Satz, Phys. Lett. 101B (1981) 89;
- [10] M. Fukugita, M. Okawa and A. Ukawa, Nucl. Phys. B337 (1990) 181.
- [11] QCDPAX Collaboration, Y. Iwasaki *et al.*, Phys. Rev. D 46 (1992) 4657.
- [12] CP-PACS Collaboration, T. Kaneko *et al.*, in preparation.
- [13] C. Allton, hep-lat/9610016.
- [14] I.R. McDonald and K. Singer, Discuss. Faraday Soc. 43 (1967) 40; A.M. Ferrenberg and R.H. Swendsen, Phys. Rev. Lett. 61 (1988) 2635; 63 (1989) 1195.
- [15] R.G. Edwards, U.M. Heller and T.R. Klassen, Nucl. Phys. B517 (1998) 377.
- [16] B. Beinlich, F. Karsch, E. Laermann and A. Peikert, Eur. Phys. J. C6 (1999) 133.
- [17] S. Ejiri, Y. Iwasaki and K. Kanaya, Phys. Rev. D58 (1998) 094505.
- [18] F. Karsch, Nucl. Phys. B (Proc. Suppl.) 60A (1998) 169.
- [19] F. Karsch, Nucl. Phys. B205 [FS5] (1982) 285.
- [20] S. Sakai, A. Nakamura and T. Saito, Nucl. Phys. B (Proc. Suppl.) 73 (1999) 417; S. Sakai, private communication.
- [21] A.D. Linde, Phys. Lett. 96B (1980) 289.

lattice	β	#iterations
$16^3 \times 4$	2.20 – 2.30	26 000
	2.32 – 3.20	20 000
16^4	2.20 – 3.20	10 000
$32^3 \times 8$	2.60 – 3.80	36 000
32^4	2.60 – 3.80	12 000

TABLE I. Statistics of our runs.

β	$16^3 \times 4$	16^4	$32^3 \times 8$	32^4
2.200	11.652966(141)	11.652657(87)		
2.250	11.856453(192)	11.855865(135)		
2.270	11.933127(336)	11.931453(117)		
2.300	12.053019(249)	12.039327(87)		
2.320	12.123597(183)	12.108015(141)		
2.350	12.221928(144)	12.206421(93)		
2.400	12.373140(177)	12.360168(129)		
2.500	12.645009(144)	12.636627(102)		
2.600	12.885558(111)	12.880320(93)	12.8802888(225)	12.8802498(198)
2.650			12.9923472(240)	12.9923202(252)
2.700			13.0990662(657)	13.0987350(177)
2.750			13.2009177(255)	13.2000711(171)
2.775			13.2497922(213)	13.2489255(162)
2.800	13.299015(138)	13.296786(99)		
2.850			13.3897845(186)	13.3890450(186)
2.900			13.4780103(183)	13.4773656(201)
3.000	13.644306(141)	13.643502(63)	13.6438083(141)	13.6433112(162)
3.200	13.938774(87)	13.938480(69)	13.9385442(174)	13.9383060(150)
3.400			14.1934539(120)	14.1933099(150)
3.600			14.4165000(162)	14.4164202(114)
3.800			14.6135793(141)	14.6135304(117)

TABLE II. Expectation value of action density $\langle S \rangle$ for our runs.

β	$a\sqrt{\sigma}$	lattice	# of conf.	Ref.
2.1508	0.5054(93)	$9^3 \times 18$	400	[3]
2.2827	0.3864(32)	$12^3 \times 24$	200	[3]
2.40	0.3096(54)	$16^3 \times 32$	50	[12]
2.5157	0.2559(23)	$18^3 \times 36$	100	[3]
2.60	0.2313(58)	$16^3 \times 32$	50	[12]
2.70	0.1963(34)	$16^3 \times 32$	100	[12]
3.20	0.1029(19)	32^4	50	[12]

TABLE III. Results for string tension obtained with the RG improved action.

$N_s^3 \times N_t$	$\beta_c(N_t, N_s)$	$\beta_c(N_t, \infty)$	$T_c/\sqrt{\sigma}$
$12^3 \times 3$	2.1528(9)	2.1551(12)	0.665(10)
$16^3 \times 4$	2.2863(10)	2.2879(11)	0.654(4)
$18^3 \times 6$	2.5157(7)	2.5206(24)	0.654(5)
$32^3 \times 8$	2.7103(32)	2.7124(34)	0.652(6)

TABLE IV. Critical coupling of the deconfinement transition for the RG improved action on an $N_s^3 \times N_t$ lattice, infinite spatial volume extrapolation and the ratio $T_c/\sqrt{\sigma}$ for infinite spatial volume. Allton's parametrization of string tension is employed to fix the temperature scale.

N_t	$p(N_t, N_s)/p_{\text{SB}}$				
	4	6	8	10	12
RG	0.1971	0.7086	0.8213	0.8734	0.9024
plaquette [4]	1.4833	1.1697	1.0748	1.0398	1.0229

TABLE V. Perturbative high temperature limit of pressure on the lattice in units of its continuum value ($p_{\text{SB}}/T^4 = 8\pi^2/45$). Results for the case $N_s/N_t = 4$ are listed.

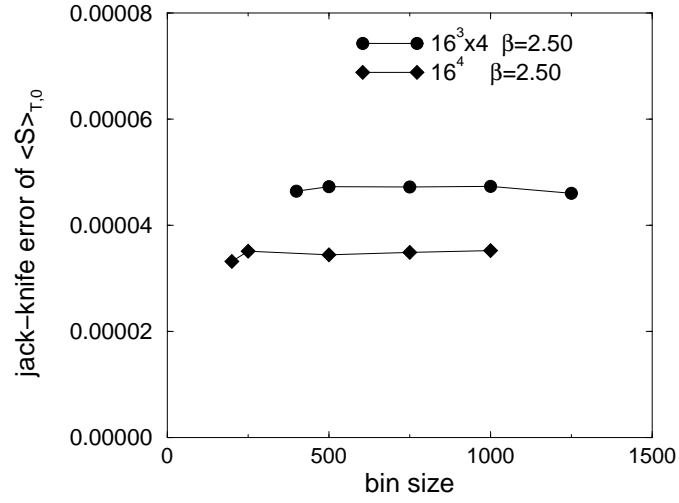


FIG. 1. Bin size dependence of the jack-knife error of the action density

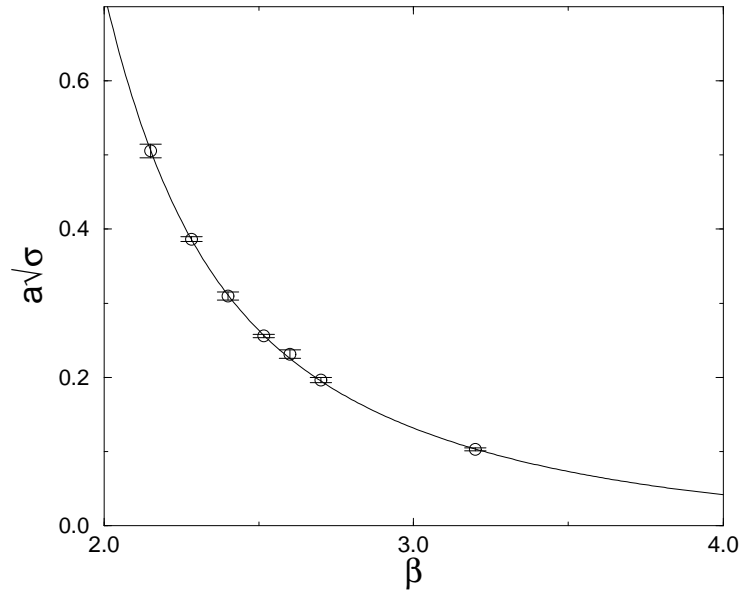


FIG. 2. String tension as a function of gauge coupling. Solid line represents a fit to Allton's parametrization.

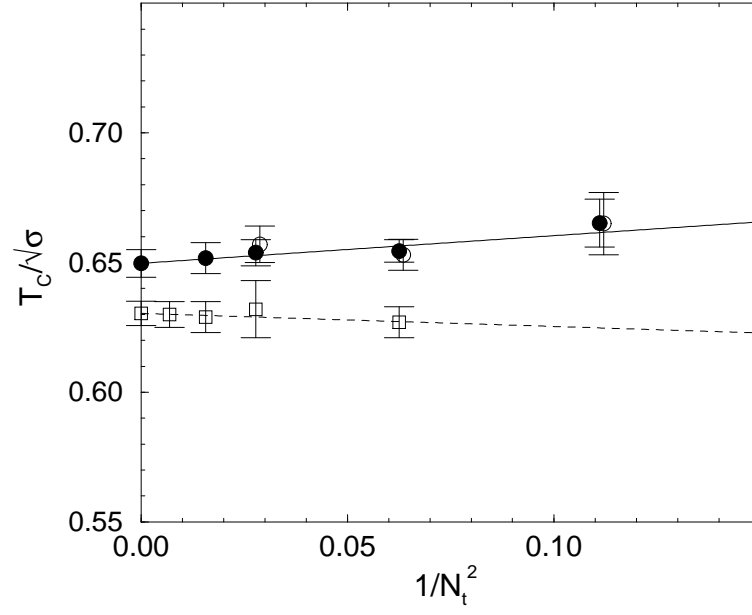


FIG. 3. $T_c/\sqrt{\sigma}$ as a function of $1/N_t^2$. Open circles are results reported in Ref. [3]. Open squares are values for the plaquette action [16].

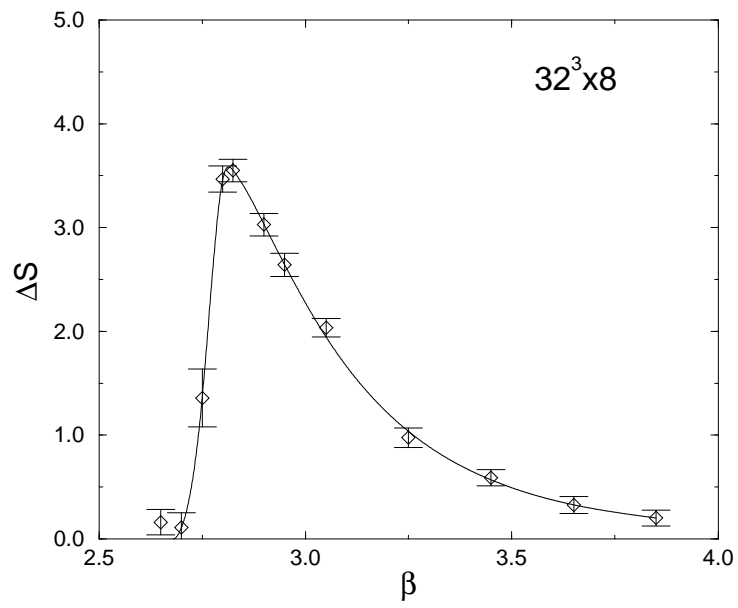
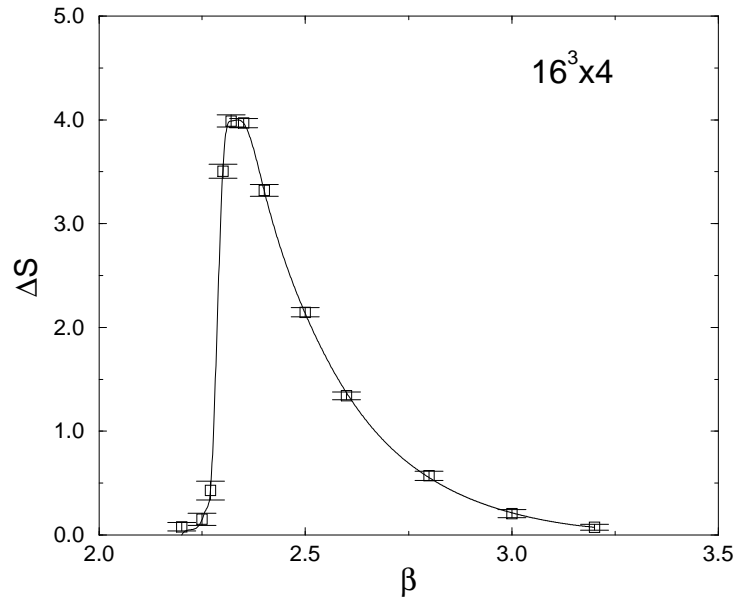


FIG. 4. Action difference ΔS for $N_t = 4$ and 8 as a function of β .

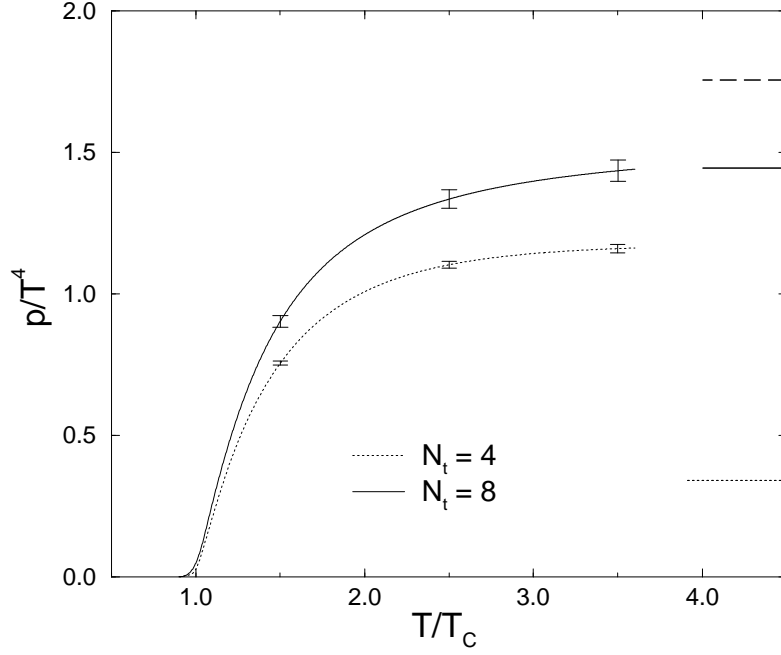


FIG. 5. Pressure for $N_t = 4$ and 8. The dashed horizontal line on the top-right represents the leading order perturbative value in the high temperature limit in the continuum, and solid and dotted lines are the corresponding lattice values for $N_t = 8$ and 4.

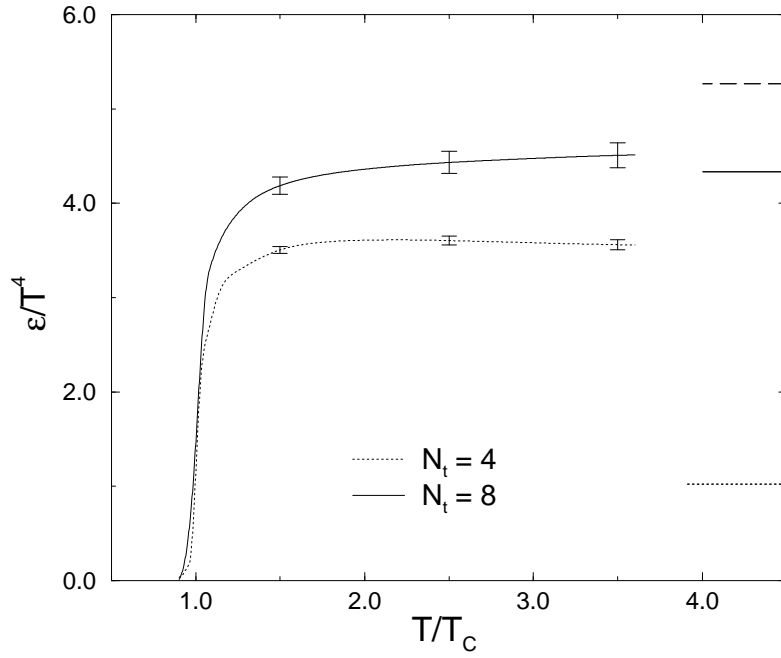


FIG. 6. Energy density for $N_t = 4$ and 8. Meaning of horizontal lines is the same as in Fig. 5

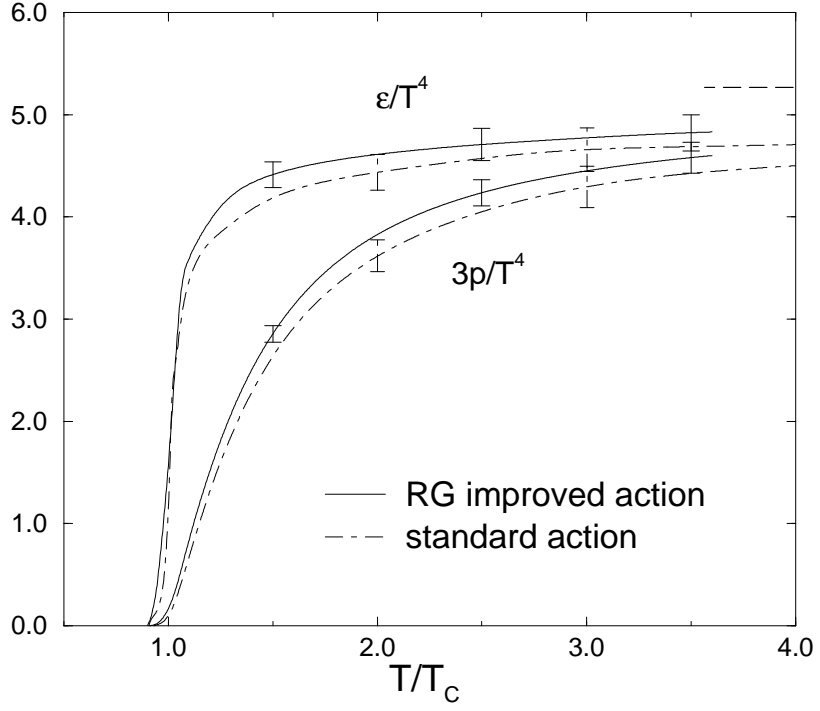


FIG. 7. Equation of state in the continuum limit for the RG-improved action (solid lines) and for the plaquette action (dash-dotted lines). The latter is obtained with the Allton's parametrization of string tension using raw data in Ref. [2]. Dashed horizontal line on the top-right shows the free gluon gas value in the high temperature limit.

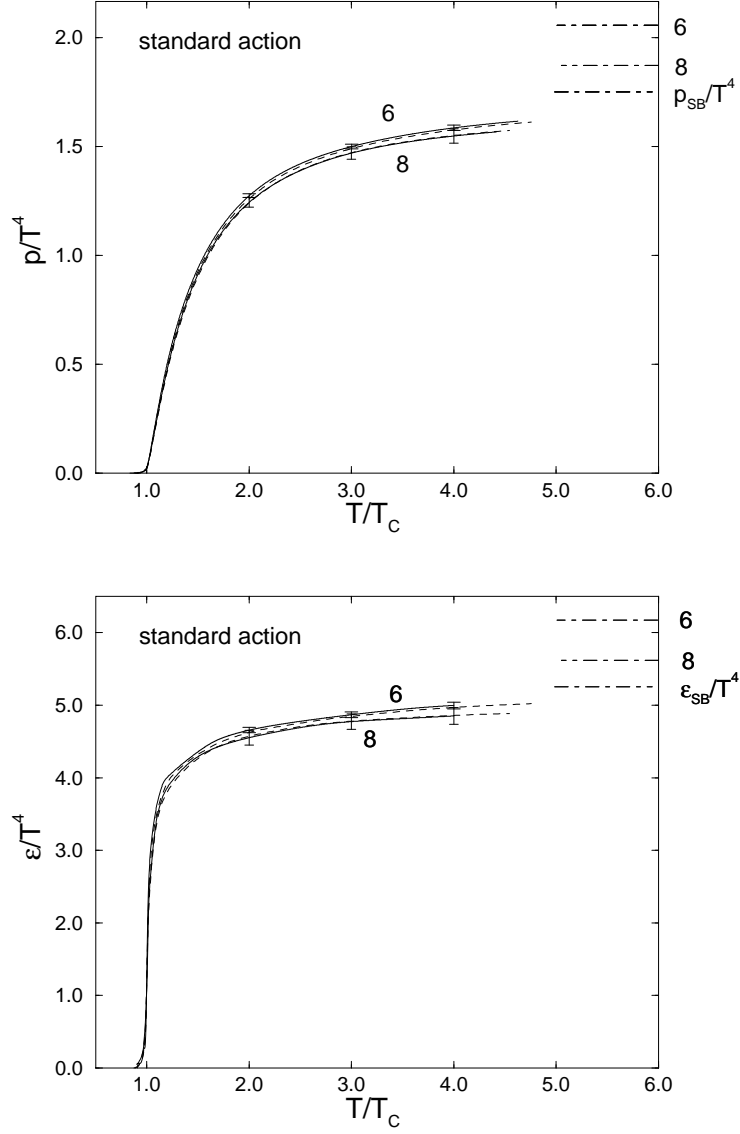


FIG. 8. Energy density (lower figure) and pressure (upper figure) for the plaquette action for $N_t = 6$ and 8. Solid lines uses the Allton's parametrization of σ for scale and dashed lines are original results of the Bielefeld group using a different scale fixing scheme.

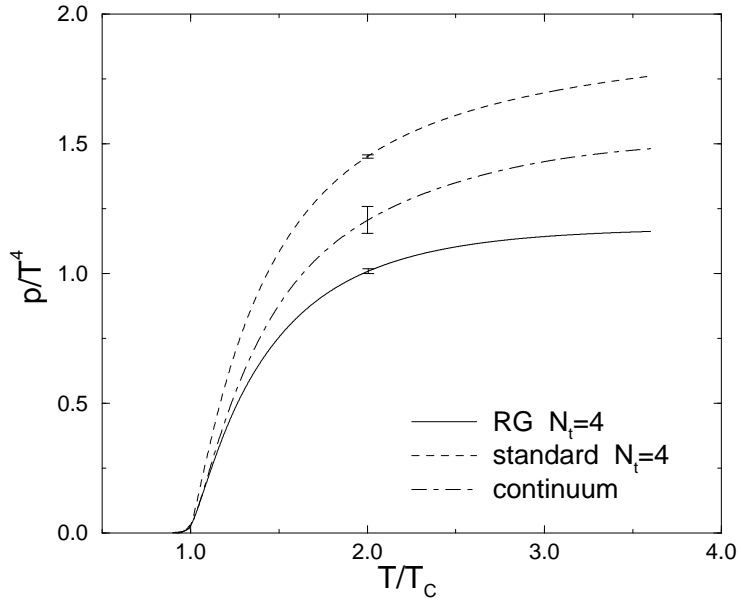


FIG. 9. Pressure at $N_t = 4$ from the RG and plaquette actions. For comparison, we also plot the result in the continuum limit obtained with the plaquette action using our choice of the scale discussed in the text.

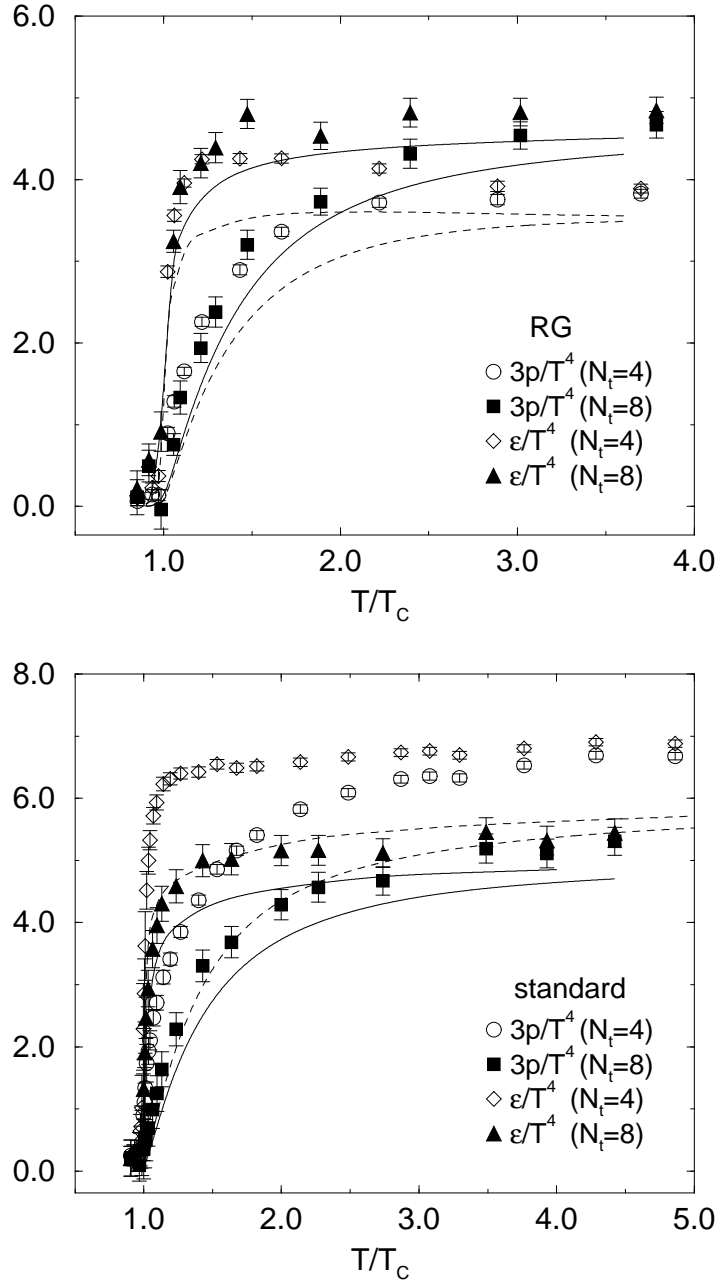


FIG. 10. Results for energy density and pressure for $N_t = 4$ and 8 obtained with the operator method using one-loop values for the asymmetry coefficients as compared with those from the integral method drawn by dashed ($N_t = 4$) and solid ($N_t = 8$) lines. Upper figure is for the RG-improved action, and lower figure for the plaquette action.